Available online at www.sciencedirect.com
SCIENCE DIRECT®
Journal of Solid State Chemistry 177 (2004) 4332–4340
JOURNAL OF SOLID STATE CHEMISTRY
www.elsevier.com/locate/jssc

SnO_2 negative electrode for lithium ion cell: in situ Mössbauer investigation of chemical changes upon discharge

I. Sandu[a], T. Brousse[a], D.M. Schleich[a], M. Danot[b,*]

[a] *Laboratoire de Génie des Matériaux, école polytechnique de l'Université de Nantes, La Chantrerie, rue Christian Pauc, BP 50609, 44306 Nantes Cedex 3, France*

[b] *Laboratoire de Chimie des Solides, Institut des Matériaux Jean Rouxel, UMR 6502, CNRS-University Nantes, 2 rue de la Houssinière, BP 32229, 44322 Nantes Cedex 3, France*

Received 12 March 2004; received in revised form 8 June 2004; accepted 9 June 2004

Abstract

In situ ^{119}Sn Mössbauer study of an SnO_2 electrode was performed during discharge of a lithium ion cell. The first step is lithium intercalation into the SnO_2 host structure. This lithium intercalation results in reinforcement of the SnO_2 lattice instead of direct decomposition of the oxide upon reduction. This first step is followed by the reduction of tin dioxide into unusual tin species (possibly "*exotic*" forms of Sn(II) or Sn(0)). The last step of the discharge consists in Li–Sn alloy formation. However, non-reduced SnO_2 is present nearly up to the end of the discharge despite a very low discharge regime. It seems highly probable that this fact is related both to slow Li diffusion and disconnection of SnO_2 particles due to Li_2O formation. The working electrode appears to be rather far from equilibrium during continuous discharge, which means that ideal succession of well-defined stages cannot describe the real phenomena involved in the operating battery.

Keywords: In situ; Mössbauer spectroscopy; ^{119}Sn; Tin dioxide; Negative electrode; Lithium ion

1. Introduction

Graphite compounds are currently the standard negative electrode in lithium ion batteries. Full lithium intercalation in graphite leads to the formation of LiC_6 [1] which provides a theoretical gravimetric capacity of 372 mAh/g. This value is quite satisfying since it is more than twice that of commonly used positive electrode materials such as $LiCoO_2$ or $LiMn_2O_4$. Despite this remarkable capacity, graphite negative electrode suffers from different problems (first cycle irreversible capacity, swelling of the electrode upon cycling, co-intercalation of electrolyte solvent, etc.), which have generated an increasing effort in the search of alternative anode materials for "rocking chair" batteries. Most of the studies aimed at solving the former problems while increasing the electrode capacity and keeping a reasonable cell voltage. The first efforts were put on tin-based oxides in the mid-1990s. In this respect, the abundant literature [2,3] (among others), including patents [4,5], devoted to SnO_2 has shown that this material exhibited promising capacity on the basis of the two-step mechanism proposed by Courtney [2]:

$$SnO_2 + 4Li^+ + 4e^- \rightarrow Sn(0) + 2Li_2O \text{ (irreversible)} \quad (1)$$

$$Sn(0) + yLi^+ + ye^- \rightarrow Li_ySn \text{ (reversible)} \quad (2)$$

According to this mechanism, the reversible specific capacity (related to the second step) of an SnO_2 electrode is about twice that of graphite (about 780 mAh/g assuming the limit formula of the Li–Sn alloys to be $Li_{17}Sn_4$, according to Nazar [6] or $Li_{22}Sn_5$, according to Huggins [7]). Since these studies, other materials have been proposed as alternative negative electrodes for Li-ion cells, with improved cyclability and

*Corresponding author. Fax: +33-2-40-37-39-95.
E-mail address: michel.danot@cnrs-imn.fr (M. Danot).

0022-4596/$ - see front matter © 2004 Elsevier Inc. All rights reserved.
doi:10.1016/j.jssc.2004.06.032

enhanced capacities. However, the strong international competition between all the proposed alternative materials has left in the shadow quite amazing features related to the solid-state chemistry of oxide electrodes, especially SnO_2.

Determination of the reaction mechanisms involved in an electrochemical system is often somewhat difficult. In particular, X-ray diffraction measurements (in situ and ex situ) have been extensively used [2,3], but they are not very informative due to the loss of long range crystalline organization which occurs as the battery works. In these conditions, use of a local technique can be very pertinent. More precisely, in the case of tin-containing electrode materials, ^{119}Sn Mössbauer spectroscopy appears as a very convenient tool [8–11]. However, most of the studies reported deal with materials which have been transferred into a Mössbauer sample holder after the battery has been stopped at a chosen stage. Even if such a procedure allows interesting conclusions to be drawn, in situ measurements carried out on an operating battery appear as much more attractive. Firstly, they avoid transfer of the material from the battery to the sample holder, an operation which can induce, even if performed under "inert" atmosphere, alteration of oxidizable phases (as we could observe by ourselves). Secondly, they allow the whole study to concern a unique battery, which suppresses the effects of possible uncontrolled differences from a battery to another. Thirdly, they permit a detailed study without requiring fabrication of a batch of batteries. Fourthly, for study of the absorption area evolution, they avoid the effects of device geometry changes, since the sample remains in the same position during the whole measurement series. For all these reasons, we decided to complete the results we obtained from our previous ex situ experiments [11] and to perform an in situ ^{119}Sn Mössbauer study of a SnO_2 electrode, in order to precise the chemical changes occurring during the discharge so that the validity of the proposed mechanism [2] is checked.

2. Experimental

It is not very convenient to perform in situ Mössbauer experiments in a glove box; the battery has thus to be sealed, in order to prevent alteration by ambient atmosphere. Moreover, presence of absorbing materials on the γ-ray beam way must be as far as possible avoided. Our battery was prepared by the Laboratoire de Réactivité et de Chimie des Solides, Unité de Prototypage UMR 6007 CNRS, Amiens, according to the plastic technology [12] which perfectly meets these requirements. Aldrich SnO_2 powder (99.9% in purity) was used. It mainly contained roughly spherical particles with diameter smaller than 1 μm (80% of the mass) but some particles reached a diameter of 40 μm. The oxide powder (active material) was mixed with poly(vinylidene fluoride)-hexafluoropropylene (PVDF-HFP), SP carbon, and dibutyl phthalate (DBP) with weight ratios 56:6:15:23, respectively. This composite electrode was not used in a real lithium ion cell but was studied as the working electrode versus a counter and reference electrode consisting of a lithium foil, which gives a well-defined reference potential. The plastic separator was soaked with a 1 M $LiPF_6$ solution in ethylene carbonate/dimethyl carbonate (EC:DMC = 1:1). A 4 cm × 4 cm piece was cut in the plastic laminate and sealed in a plastic bag in order to be used as the Mössbauer sample.

The battery discharge, i.e. the reducing step (3 weeks) was monitored by a MacPile device operating according to the potentiostatic mode. The potential was varied step by step and the current continuously measured in order to allow, through integration, determination of x, the mole number of lithium having reacted from the beginning of the discharge with one mole of SnO_2.

Three potential steps were used for the first discharge of the battery. Up to $x = 0.5$ Li, the potential was varied by stage of −10 mV per hour. Between $x = 0.5$ and 3.8 Li (corresponding to the pseudo plateau formation, cf. Fig. 1a) the cycling mode was slowed down, i.e. to −10 mV per 10 h. For x values higher than 3.8 Li and until the end of the discharge, the potential stages were −10 mV per 3 h.

The Mössbauer measurements were performed using a conventional constant acceleration spectrometer equipped with a $Ca^{119m}SnO_3$ source (5 mCi). The velocity scale was calibrated with two reference absorbers, β-Sn and $CaSnO_3$. The isomer shifts are referred to $CaSnO_3$ at room temperature. The typical acquisition time was about 24 h per spectrum. The amount of reacted lithium (x Li per SnO_2 mole) corresponding to each of the spectra (and used in the text and the figures) is calculated as the average value between the lithium amounts at the beginning and at the end of the acquisition time.

All the in situ spectra were of course recorded at room temperature. It has to be kept in mind that, for such a high measuring temperature, some difficulties can be encountered concerning identification of phases with a low recoilless fraction (f, Lamb-Mössbauer factor) and determination of the relative amounts of phases with different f-values.[1]

[1]Only the f fraction of the ^{119}Sn nuclei participates in the Mössbauer spectrum since Mössbauer effect is based on recoilless resonant absorption of γ-rays by nuclei. The $(1-f)$ remaining fraction dissipates the total recoil energy of the system as lattice vibrations and thus cannot contribute to the resonant absorption. The recoilless fraction reflects the dynamics of the tin-containing lattice. At a given measurement temperature, it is higher if the lattice is more rigid, i.e. if Sn is involved in strong bonds. For a given compound, decrease of

3. Results and discussion

As pointed out above our aim was to fully detail the electrochemical behavior of a SnO_2 electrode in a lithium ion cell using in situ ^{119}Sn Mössbauer spectroscopy. For clarity, we will successively address the different reaction steps in order to give some clues to elucidate the anomalies detected.

3.1. Does the equation $SnO_2+4Li^+ +4e^- \rightarrow Sn(0)+2Li_2O$ really reflect the first step of the discharge?

3.1.1. The lowest Li contents

Up to $x \approx 0.4$ Li having reacted with one mole of SnO_2, the Mössbauer spectra remain visually identical to the broadened singlet (unresolved quadrupole doublet) of the SnO_2 starting material, without any extra contribution to be observed (Fig. 1b and c). It can then be thought that, at this stage, the reaction does not induce deep changes of the SnO_2 electrode, i.e. no important change of the strong bonds occurs. However, the absorption area normalized to the background count number (NormAbs) exhibits a rather unexpected trend for the lowest x values, since it increases with x (up to $x \approx 0.2$, Fig. 2). This trend is unexpected because, according to Eq. (1), SnO_2 should transform into metallic tin. The contribution of these new species to the Mössbauer spectra could be unobservable due to low recoilless fraction, but decrease of the SnO_2 amount should necessarily induce decrease of the absorption area, as unambiguously observed above $x \approx 0.2$ (Fig. 2). The absorption area should then monotonously decrease with increasing x, including the lowest x values. It means that Eq. (1) does not represent the phenomenon occurring at the very beginning of the discharge.

For such spectra with a unique tin contribution, the normalized absorption area (NormAbs) is proportional to the N number of tin nuclei present in the sample and to their f recoilless fraction. The NormAbs increasing from $x = 0$ to 0.2 (Fig. 2) can result from an increase in N because only part (3 cm^2) of the electrode surface is exposed to the collimated γ-ray beam so that, if the lattice and consequently the electrode contract, the number of tin atoms in the measurement area may increase. Nevertheless, electrode contraction could rather be expected to result in formation of cracks without important change of the tin active amount. Moreover, the NormAbs increase from $x = 0$ to 0.2 is

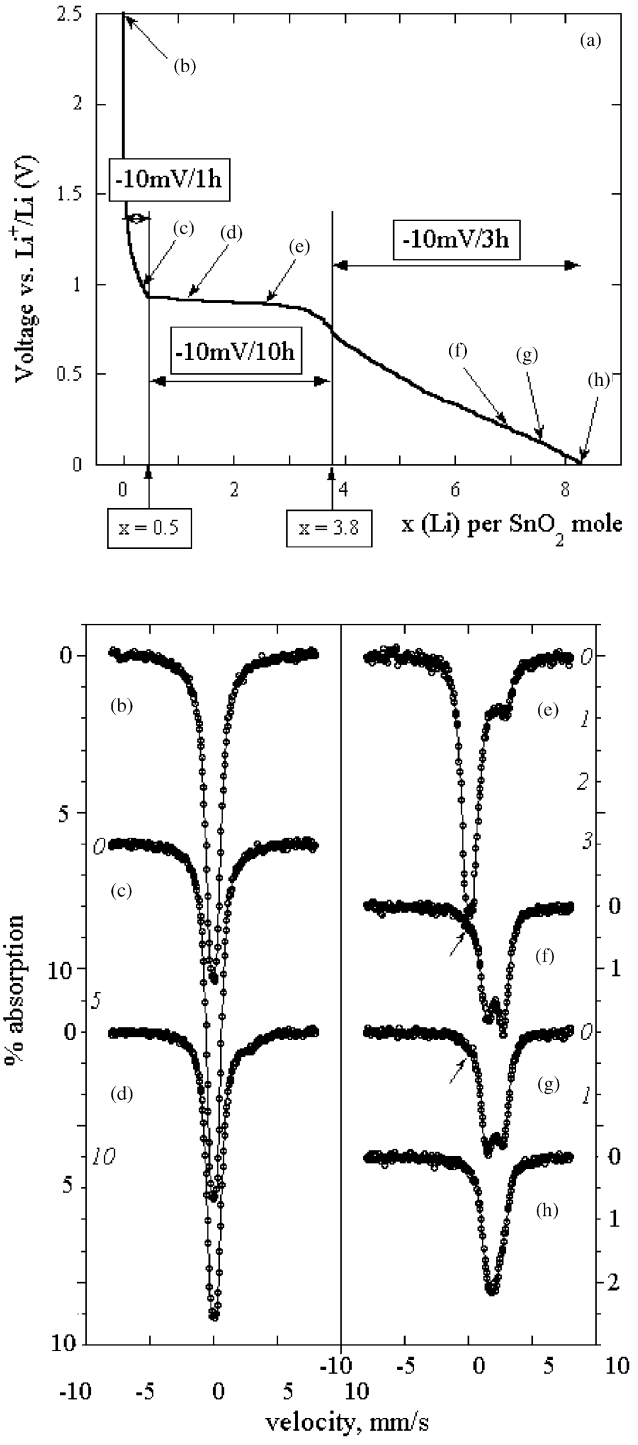

Fig. 1. (a) First potentiostatic discharge of the SnO_2 electrode between open circuit voltage (OCV) and 0.01 V vs. Li^+/Li. (b)–(h) In situ ^{119}Sn Mössbauer spectra recorded at different x values ($x = 0.00$ (*b*), 0.39 (*c*), 1.26 (d), 2.63 (*e*), 6.90 (*f*), 7.56 (*g*), 8.40 (h)) during the first discharge of the electrode. For clarity purpose, plain and italic types are alternately used for (*b*), (*c*), (d), (*e*), (f), (*g*), (h), and for the corresponding absorption scales. It should be noted that the absorption scale for spectra (*e*), (f), (*g*), (h) is twice as large as that for spectra (b), (*c*), (d), which illustrates the drastic drop of the overall f factor upon discharge. The contribution of residual SnO_2 traces to spectra (f) and (*g*) is indicated by the arrows.

(*footnote continued*)
the measurement temperature attenuates the lattice vibrations and thus increases f. If tin is present in proportions $p(i)$ in several (i) species in a sample which contains a total of N tin atoms, the contribution of each of these species, Abs(i), to the total absorption area (AbsTot = ΣAbs(i)) is proportional to $p(i) \times N \times f(i)$. For this reason, the $p(i)$ proportions of tin in the different species can be deduced from the corresponding Abs(i) areas only if the $f(i)$ values are known.

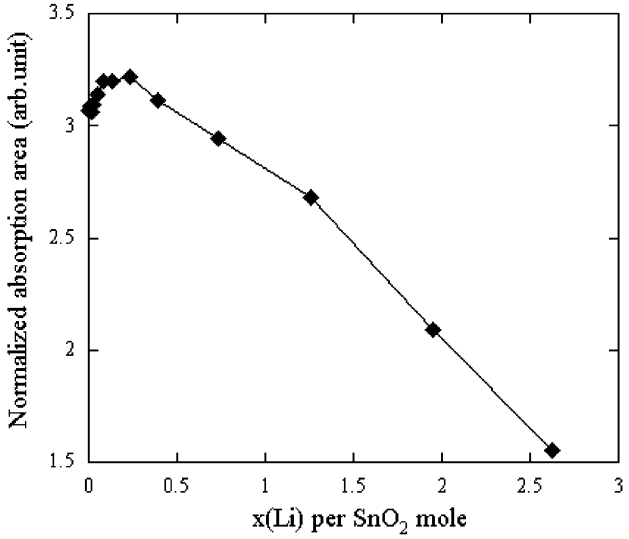

Fig. 2. Variation of the absorption area (normalized to the background count number) versus x, the Li amount per SnO_2 mole ($0.00 \leqslant x \leqslant 2.63$). (*The line is a guide for the eyes.*)

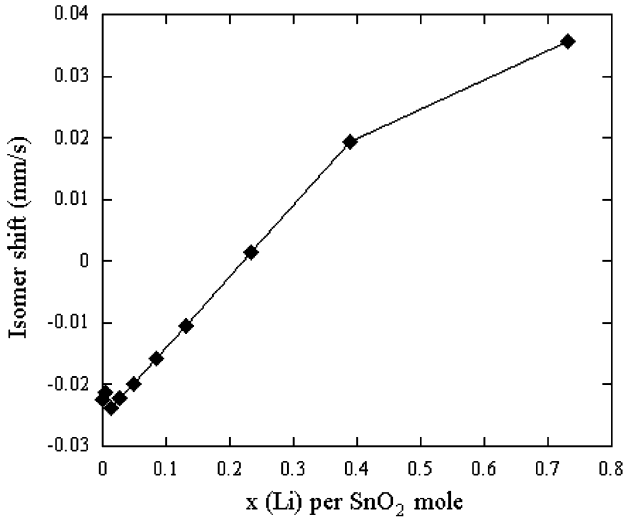

Fig. 3. Evolution of the ^{119}Sn isomer shift (δ) versus x, the Li amount per SnO_2 mole ($0.00 \leqslant x \leqslant 0.73$). (*The line is a guide for the eyes.*)

about 5% which would require notable lattice contraction. Now, ex situ recorded X-ray diffractograms did not evidence any significant lattice parameter change in this region. The only possibility is then that the NormAbs increase is due to an increase in f, which means that the SnO_2 lattice becomes more rigid. Such a phenomenon can be explained by lithium intercalation into the host SnO_2 lattice, with creation of new bonds (Li–O) without destruction of the pre-existing ones (Sn–O), which thus results in reinforcement of the lattice. Besides, in this composition region, the tin isomer shift slightly increases with x ($\delta = -0.02$ mm/s for $x = 0$, and $\delta = 0.00$ mm/s for $x = 0.2$). This increase is not far from the limit of experimental accuracy, but it is in agreement with what can be expected for oxygen-surrounded tin (IV) in the presence of a more electropositive cation [13].

At the beginning of the discharge (Fig. 1a), a drastic potential drop is first observed (from 0 to 0.5 Li per SnO_2 mole), followed by a pseudo plateau, which demonstrates that two different phenomena occur in this region. The first one can then be attributed to lithium intercalation into the SnO_2 host, the second one to reduction of the lithiated structure. However, intercalation finishes at $x = 0.5$ according to the voltamogram, while the maximum of the Mössbauer absorption area is located at $x = 0.2$. The NormAbs decrease above $x = 0.2$ can be explained by reduction of more or less lithiated SnO_2 into species with a smaller f factor. It can thus be thought that reduction begins at $x = 0.2$ (absorption area), while intercalation is still going on (voltamogram). This hypothesis is supported by the fact that the isomer shift of the SnO_2-related contribution continues to increase above $x = 0.2$ (Fig. 3), which suggests that, as the lithiated phase begins to be reduced, further lithium intercalation proceeds in non-reduced parts of this phase.

It thus appears that the first step of discharge is not reduction of SnO_2 into metallic Sn, but lithium intercalation into the SnO_2 lattice.

3.1.2. Evolution of the remaining SnO_2 fraction during the battery discharge

The absorption at $v \approx 0$, characteristic of more or less lithiated SnO_2, remains observable for lithium amounts higher than $x = 4$, the value expected according to the mechanism proposed by Courtney [2]. The relative contribution of this sub-spectrum to the total absorption in a given spectrum cannot allow to determine the effective proportion of SnO_2 at the corresponding stage, since the f factors of the various species involved are not known. However, we could estimate the proportion of unreacted SnO_2 as follows. For each of the spectra recorded during the battery discharge, we calculated the absorption area relative to the SnO_2 contribution and normalized it with respect to the background count number. The remaining SnO_2 fraction (F_{SnO_2}) was then calculated by dividing each of these values by that obtained for $x = 0$, which corresponds to $F_{SnO_2} = 1$. This procedure gives for $0 < x < 0.4$ F_{SnO_2} fractions slightly greater than 1 (up to 1.05) due to the initial absorption area increase. Such values are of course meaningless. For this reason they have been arbitrarily replaced in Fig. 4 by the maximum possible value, 1. Anyway, this minor point cannot change anything

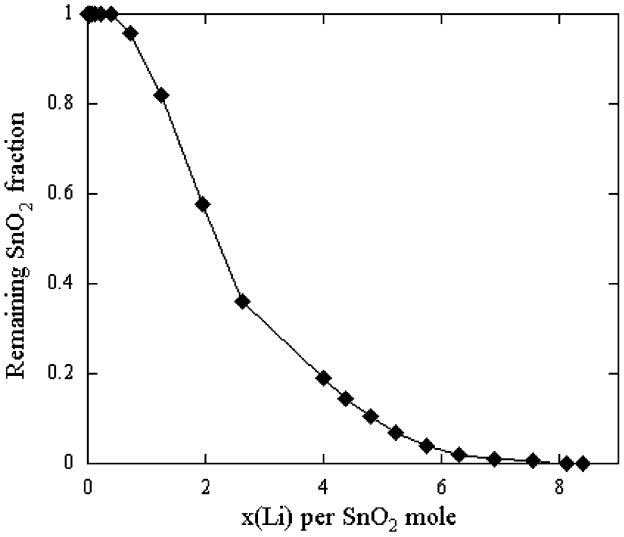

Fig. 4. Evolution of the remaining SnO_2 fraction during the electrode discharge. (*The line is a guide for the eyes.*)
The uncertainty on the estimated fractions of unreduced SnO_2 is about 5%. For the high Li amounts ($x = 6.90$ for instance), even if the unreduced SnO_2 fraction is very small (0.01), its presence is not questionable since its contribution clearly appears at $v \approx 0$ as a shoulder on the left wing of the doublet (cf Fig. 1f).

owing to the conclusion that some SnO_2 remains present in the electrode nearly till the end of the discharge (Fig. 4). It can be thought that the remaining SnO_2 does not exactly correspond to the usual tin dioxide. Effectively, the isomer shift related to this sub-spectrum continues to increase with x (as shown by Fig. 3) up to ≈ 0.16 mm/s. Even if δ determination becomes less accurate when the corresponding contribution becomes less intense, due to correlations with the parameters of the other components of the unresolved spectra, this value is consistent with that we obtained from ex situ spectra recorded at 78 K (0.19 mm/s [11]). Such a δ increase probably means that, as proposed above, intercalation goes on while reduction proceeds, as long as SnO_2 is present. This phenomenon could result from the presence of SnO_2 regions where lithium access is sufficient for intercalation to occur, but too slow for Sn(IV) to be immediately reduced. However, such δ values could also be related to SnO_2 regions in interaction with surrounding Li_2O particles.

Anyway, again it appears that ideal succession of well-defined stages cannot describe the real phenomena involved in the operating battery.

3.2. The chemical evolution of the system

3.2.1. The first reduction step

As indicated above, after the maximum at $x = 0.2$, the normalized absorption area drastically decreases (Fig. 2) which means that SnO_2 transforms into new species with lower f factor. Due to this small recoilless fraction, the contribution of these new species become perceptible only for $x > 1$ (Fig. 1) and, even for $x > 2.5$, it remains weak if compared to that of the remaining SnO_2. Besides, the various sub-spectra are not resolved, and strong correlations between the parameters to be refined make it difficult to propose unambiguous identification of the reaction products up to $x = 3.6$. Satisfactory reproductions of the spectra can be obtained without β-Sn contribution and, if we introduce such a contribution (which was observed in our previous ex situ 78 K measurements [11]), its intensity is weak, which can be due to the very low f value expected for small particles of β-Sn. Whether β-Sn is considered or not, at least another contribution exists, with an isomer shift of about 2.2 mm/s which corresponds neither to β-Sn ($\delta = 2.56$ mm/s [14]) nor to SnO ($\delta = 2.62$ mm/s [15]). This cannot be explained on the basis of the ex situ spectra we previously recorded at 78 K [11]: effectively, during the discharge, we clearly observed coexistence of β-Sn and Sn (IV) (without significant amount of Sn(II)). Low temperature enhancement of the β-Sn f factor can explain β-Sn contribution to be observable at 78 K (ex situ) and not at room temperature (in situ), but it cannot justify the presence of new contribution(s) in the room temperature in situ spectra. It can then be thought that unusual species transitorily form; they could be evidenced by the in situ study but could transform into a more stable phase during the time between when the battery was stopped and our ex situ spectra [11] recorded (at least several days of room temperature annealing). In this respect, the isomer shift value ($\delta \approx 2.2$ mm/s) observed in the in situ spectra is intermediate between those of α-Sn (2.0 mm/s) and β-Sn (2.56 mm/s) and close to that reported for tin thin films (2.25 mm/s) [14]. The reduction product observed in situ could then correspond to some unusual form of metallic tin, which could then transform into the β-Sn observed ex situ. However, such a δ value could also be related to an unusual form of Sn(II). In both cases, the species can possibly be in interaction with Li_2O.

3.2.2. Alloy formation

The following step of the discharge (from $x \approx 4$) can be expected to involve formation of Li_ySn alloys [2], as already evidenced by our ex situ study [11]. In this region, our in situ spectra consist (apart from the contribution of nonreduced Sn(IV)) of a more or less symmetrical doublet with broadened lines, whose simulation obviously requires more than one tin site. An extensive study of the Li–Sn system reported by Dunlap et al. [16] shows that several phases exist, with several tin sites for most of them. Since an ideal step by step mechanism is not followed (as demonstrated above), coexistence of several alloy phases in the electrode can be anticipated which means that each of the corresponding spectra can contain a rather large

number of contributions. However, considering that these various contributions are unresolved, we thought it would not be very significant to introduce in our calculations an excessive number of variables. For this reason, we used the minimum number of tin sites required for good reproduction of our experimental spectra: two sites, plus the contribution of unreacted Sn(IV).

Fig. 5 gives the evolution of the Mössbauer parameters of the two alloy tin sites versus the Li/Sn atomic ratio in the Li_ySn alloys. For the y value to be really representative of the alloy composition, it has been calculated according to F_{SnO_2}: $y = x - 4(1 - F_{SnO_2})$, where x is the total lithium amount involved from the beginning of the discharge and $4(1 - F_{SnO_2})$ the lithium amount effectively involved in reduction of SnO_2 into metallic Sn, taking into account the F_{SnO_2} fraction of unreduced SnO_2 (cf. Fig. 4). The lithium amount possibly intercalated in the unreduced SnO_2 was not introduced in this calculation of y because it cannot be reliably estimated; anyway this cannot induce important error on the y value.

For the two sites, the isomer shift decreases with increasing lithium amount. This evolution reflects progressive replacement of Sn–Sn contacts (Li-poor alloys) by Sn–Li ones (Li-rich alloys), in agreement with the Li–Sn system study of Dunlap [16]. Now with regard to the quadrupole splitting evolution, it can be seen (Fig. 5) that the site with the greatest isomer shift has first the smallest quadrupole splitting and that the situation reverses above $x \approx 7$. This crossover is related to the change of the doublet asymmetry: the line located at the lowest velocity is first less intense (Fig. 5f) and, above $x \approx 7$ (Fig. 5g), becomes more intense than the line located at the highest velocity. Similar change of the spectra asymmetry was observed by Dunlap between Li_7Sn_3 and Li_5Sn_2 [16]. It can thus be thought that some similarity exists between the species we formed and the alloys described by Dunlap. However, they are not perfectly identical since the isomer shift and quadrupole splitting values we refined in this region (Fig. 5) are somewhat different (slightly greater) than those reported by Dunlap for the corresponding well-defined Li_7Sn_3 and Li_5Sn_2 alloy phases. These differences can be due to poorer organization and/or non-stoichiometry of our alloy particles.

Our two site fitting procedure perhaps does not describe exactly the studied electrode (which procedure could be indisputable for such unresolved spectra?); however, it allows calculating for each spectrum the mean isomer shift value (weighted on the basis of the relative contributions of the two sites to the absorption area). An interesting feature is that, for spectra which can be reproduced according to different hyperfine parameter sets, the mean isomer shift value does not depend upon the chosen model (which is not surprising since this value represents the spectrum barycenter). Fig. 6 shows the evolution of the alloy mean isomer shift versus the y Li/Sn atomic ratio (calculated taking into account the amount of unreduced SnO_2 as in Fig. 5). Along with our results and for comparison purpose, Fig. 6 also gives the tin mean isomer shift values calculated from the data reported by Dunlap for well-organized Li–Sn alloys [16] and by Chouvin for

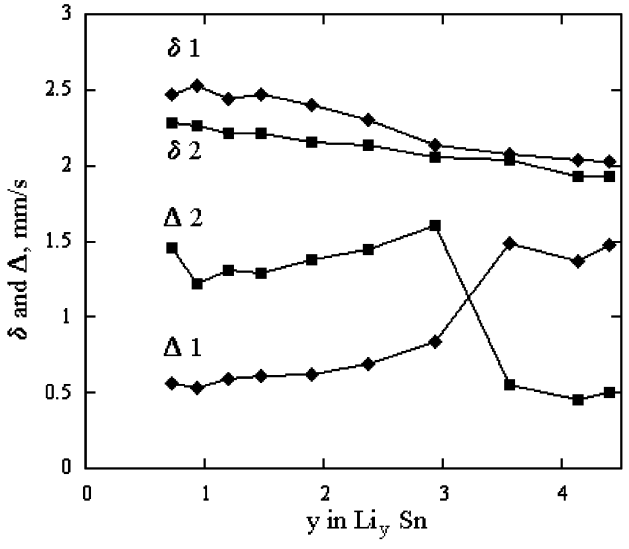

Fig. 5. Two-site description of the Mössbauer spectra of the Li_ySn alloys: evolution of the ^{119}Sn isomer shifts ($\delta 1$, $\delta 2$) and quadrupole splittings ($\Delta 1$, $\Delta 2$) versus y. (*The lines are guides for the eyes.*)
The uncertainty on δ and Δ values is 0.04 mm/s. The data refined for the lowest Li content are probably affected by presence of residually reduced but non-alloyed species.

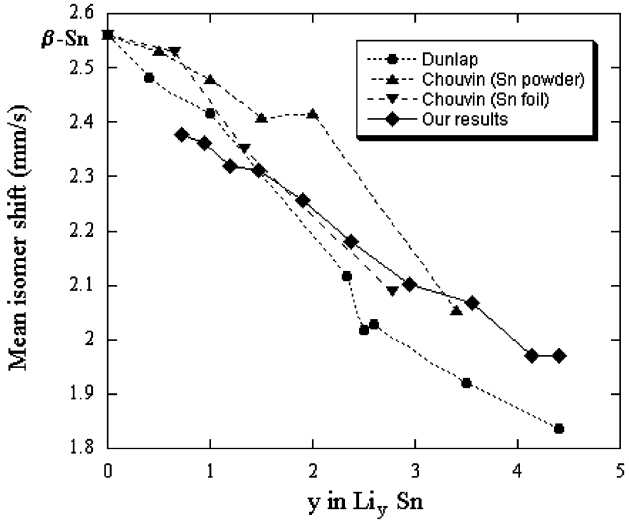

Fig. 6. Two-site description of the Mössbauer spectra of the Li_ySn alloys: evolution of the ^{119}Sn mean isomer shift (δ) versus y. Results derived from Dunlap and Chouvin data are given for comparison. (*The lines are guides for the eyes.*)

electrochemically obtained ones (two data sets for two different morphologies of the β-Sn starting material [10]). We have considered the δ value of β-Sn (2.56 mm/s) to belong to the three curves drawn from the results of Dunlap and Chouvin because in these three cases β-Sn is the starting material. For the four measurement series, the overall trend is similar: the mean δ-value decreases as the Li/Sn ratio increases, i.e. as Sn–Sn contacts are replaced by Sn–Li ones. However, the four curves are not identical. For low lithium contents, our δ-values are smaller than those of Dunlap and Chouvin, and do not extrapolate to $\delta = 2.56$ mm/s (β-Sn) for $y = 0$. For high lithium contents, our δ-values are greater than those of Dunlap (comparison to the results of Chouvin is less significant because his lithium-rich alloy corresponds to Li/Sn = 3.4, instead of 4.4 for our alloys and those of Dunlap). These differences can probably be explained, at least partly, by different synthesis procedures. Dunlap obtained well-defined alloys from the elements at high temperature, which can be enough to account for differences with our results. Differences with the values of Chouvin are more surprising since Chouvin's study concerns, as ours, electrochemically prepared alloys. Of course, the starting materials are not the same, β-Sn for Chouvin, SnO_2 for us, but, as far as SnO_2 can be expected to be first reduced into β-Sn or any unusual form of metallic tin, it could be thought that no significant difference should exist between the three series. However, it has to be noticed that, for the same starting material (β-Sn), the two curves for the Chouvin's alloys are different depending on the β-Sn morphology, powder or thin film. It follows that, if β-Sn is formed through reduction of our SnO_2 electrode, it has no reason to exhibit a morphology identical to that of one of the starting materials of Chouvin. In fact, we did not unambiguously evidence formation of β-Sn, possibly due to its low recoilless fraction. As far as the contribution we observed with $\delta \approx 2.2$ mm/s is really related to an unusual form of metallic tin, the resulting Li–Sn alloys could exhibit an unusual form too.

Moreover, for discussion of the plot versus y of the mean isomer shift of tin in our alloys (Fig. 6), it has to be kept in mind that our measurements concern a working system which does not follow an ideal equilibrium mechanism, as shown by the persistence of unreduced Sn(IV) far above the theoretical value of 4 Li per SnO_2 mole. In these conditions, the Li–Sn alloys present at any moment have no reason to be homogeneous, which can have consequences concerning the estimation of the mean isomer shift value due to the dependence of the tin recoilless fraction upon the composition of the alloys. Effectively, in a first approach, for measurements performed at a given temperature (room-temperature in the present case) the f factor can be anticipated to increase with the material melting point (expected to vary in the same way as the lattice rigidity), i.e. to first increase with the Li/Sn ratio and then slightly decrease for the highest Li contents [9,17]. In order to check this assumption, we have studied the evolution of the absorption area related to the alloys versus their composition, represented by the Li/Sn ratio, y (as calculated for Figs. 5 and 6). For each spectrum, the absorption area relative to the alloys (AllAbs) is calculated by addition of the absorption areas relative to the two alloy tin sites. This AllAbs value is divided by the background count number for normalization of the different spectra (NormAllAbs). For one mole of SnO_2 initially present in the electrode, the amount of tin effectively involved in the Li–Sn alloys is $F_{All} = 1 - F_{SnO_2}$ (F_{SnO_2} is the fraction of unreduced SnO_2 as plotted in Fig. 4). The normalized alloy absorption referred to one Sn involved in the alloys is then NormAllAbs per Sn = NormAllAbs/F_{All}. Since they refer for all the spectra to the same Sn number, these NormAllAbs per Sn values are then proportional to the recoilless fractions related to the different Li_ySn compounds. Fig. 7 shows that, as expected from the melting points evolution, NormAllAbs per Sn first drastically increases and then slightly decreases. It means that the f factor severely depends upon the alloy composition. Let us consider an inhomogeneous alloy system with two components named Li-poor ($y = 1$ for instance) and Li-rich ($y = 2$ for instance) in relative proportions $F_{Li\text{-}rich}$ and $F_{Li\text{-}poor}$. The absorption area ratio, $Abs_{Li\text{-}poor}/Abs_{Li\text{-}rich}$, will be given by $(F_{Li\text{-}poor} \times f_{Li\text{-}poor})/(F_{Li\text{-}rich} \times f_{Li\text{-}rich})$. Since $f_{Li\text{-}poor} < f_{Li\text{-}rich}$ ($f_{Li\text{-}poor}/f_{Li\text{-}rich} \approx 0.7/0.8$, cf. Fig. 7) the $Abs_{Li\text{-}poor}/Abs_{Li\text{-}rich}$ ratio will be smaller than the $F_{Li\text{-}poor}/F_{Li\text{-}rich}$ amount ratio,

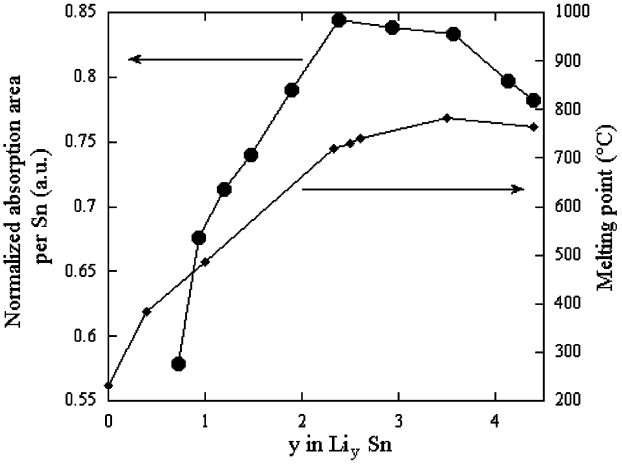

Fig. 7. Melting points reported in the literature for well-defined Li_ySn alloys, and normalized absorption area per Sn mole involved in the Li_ySn alloys formed in our electrode. For comparison, before the battery begins to work, the normalized absorption area for the SnO_2 spectrum is greater than 3 in the same arbitrary unit system. It shows the drastic decrease of the overall f factor. (*The lines are guides for the eyes.*)

which really represents the systems. It follows in such a case that calculation of the mean isomer shift of the alloys, weighted on the basis of the $Abs_{Li\text{-}poor}/Abs_{Li\text{-}rich}$ ratio, will under-estimate the participation of Li-poor and over-estimate that of Li-rich. Since the isomer shift decreases with increasing Li content ($\delta_{Li\text{-}poor} > \delta_{Li\text{-}rich}$), this procedure will somewhat under-estimate the mean isomer shift value in this region. This effect cannot be quantified, but it is sure that if it could be, the curve we would obtain would be less different from those derived from the results of Chouvin and Dunlap. For the highest lithium contents, when NormAllAbs per Sn decreases with increasing y (Fig. 7) symmetrical trend can be expected for f, but less important since the decrease of NormAllAbs per Sn is much less important above $y \approx 2.5$ than from $y \approx 2.5$ to $y = 0$. Nevertheless, the result would then be that, in this case, our mean isomer shift value is over-estimated. If this phenomenon could be taken into account, our curve would be closer, in this region too, to the three other ones. Moreover, the NormAllAbs per Sn versus y plot (Fig. 7) suggests the f value for metallic Sn to be very low, which can explain the related contribution not to be observable in the spectra, despite the presence of β-Sn was evidenced from ex situ X-ray diffraction and low temperature Mössbauer measurements [11].

This discussion shows that interpretation of room temperature in situ Mössbauer experiments is not necessarily straightforward. However, it one more time points out that the working electrode is anything but homogeneous.

3.3. What happens when the cell is discharged?

The first factor which can explain that some SnO_2 remains unreduced above the expected $x = 4$ limit is lithium diffusion in the SnO_2 structure. In order to check this hypothesis, estimation has been made concerning the lithium diffusion coefficient D_{Li} ($D_{Li} = r^2/t$, r being the particle radius (cm) and t the reaction time (s)). For this estimation, we have chosen $t = 10^6$ s (12 days), which is the time passed between the beginning of the discharge and recording of the spectrum corresponding to $x = 4$. Effectively, at this stage, 80 wt% of SnO_2 is reduced ($F_{SnO_2} = 0.2$, cf. Fig. 4), which is precisely the weight percentage of SnO_2 particles with a diameter less than 1 μm. For these small particles to be completely reduced, a D_{Li} coefficient of 2.5×10^{-15} cm^2/s is sufficient. In the rutile structure, the D_{Li} coefficient has been reported to range between 10^{-6} and 10^{-12} cm^2/s [18]. It thus appears logical that the small particles are completely reduced. For the largest SnO_2 particles (up to $d = 40$ μm) to be completely reduced too, the D_{Li} coefficient should be at least 4×10^{-12} cm^2/s. This value is of the same magnitude order as the smallest D_{Li} value reported for rutile structure. Assuming lithium diffusion in our SnO_2 particles to be effectively among the slowest in rutile structure, this phenomenon could be (partly?) responsible for the presence of unreduced SnO_2 in the largest particles.

Another reason for this presence can be related to Li_2O formation. Li_2O can be expected to form at the surface of the SnO_2 particles and can so constitute an insulating barrier, which impedes lithium access to the unreduced core of the particle. Then, during discharge, and especially when the Li–Sn alloys appear, considerable material expansion occurs since the complete transformation of the active phase results in a volume increase of 300%. This volume increase necessarily induces important mechanical strains, which can grind the Li_2O particles and thus restore contact between the remaining SnO_2 and the reactional medium, which allows the SnO_2 reduction to start again (Fig. 8). Even if further experiments with fine SnO_2 powder as the starting material would be necessary for unambiguous answer to be given, it seems highly probable that both phenomena (Li diffusion and disconnection-reconnection of the SnO_2 particles) are responsible for persistence of unreduced SnO_2 nearly until the end of the discharge.

Finally, our measurements allow describing the phenomena involved during the battery discharge according to Fig. 9, which shows the imbrications of the various reactions.

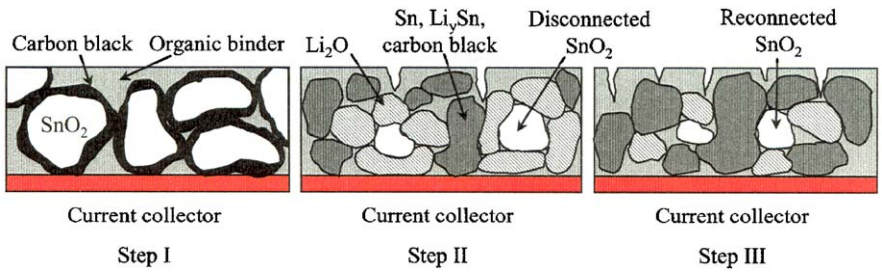

Fig. 8. Disconnection–reconnection of the SnO_2 particles due to Li_2O formation and further grinding of these particles related to the alloy formation and concomitant volume expansion. Binder: poly(vinylidene fluoride)-hexafluoropropylene (PVDF-HFP); conductive additive: SP carbon. See experimental section for electrode composition.

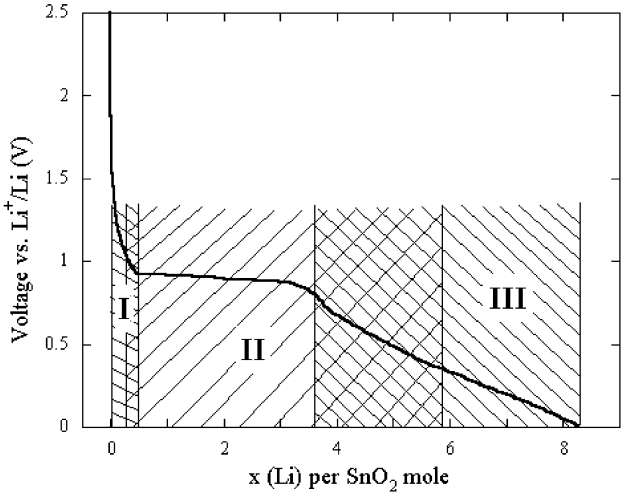

Fig. 9. Various mechanisms taking place during the first discharge of the SnO_2 electrode: lithium intercalation into the SnO_2 host structure (I), reduction of the more or less lithiated SnO_2 (II), Li_ySn alloy formation (III).

4. Conclusion

Even if the spectra were recorded at room temperature, in situ Mössbauer ^{119}Sn spectroscopy allowed better understanding of the behavior of the SnO_2 electrode during the battery discharge. In particular, the first part of the voltametric curve could be explained on the basis of lithium intercalation in the SnO_2 host structure, and it could be evidenced that the succession of well-defined stages previously proposed does not exactly represent the phenomena really involved in our system. Additionally, this study brings new insights on the use of SnO_2 in electrochemical devices. For example, lithium intercalation can be used for electrochromic purpose for example, and the study of Li_xSnO_2 solid solution can be interesting from both fundamental and applied points of view. Besides, the present study points out the influence of particle size distribution on the electrochemical properties of batteries. Subsequently, the battery performance can be monitored via electrode material engineering.

Acknowledgments

The authors would like to thank Dr. Mathieu Morcrette from Laboratoire de Réactivité et de Chimie des Solides, Unité de Prototypage UMR 6007 CNRS, Amiens, for the cell preparation. Dr. Philippe Deniard and Dr. Dominique Guyomard (Laboratoire de Chimie des Solides, Institut des Matériaux Jean Rouxel) are also acknowledged for their help with the electrochemical tests.

References

[1] D. Guérard, A. Herold, Carbon 13 (1975) 337.
[2] I.A. Courtney, J.R. Dahn, J. Electrochem. Soc. 144 (1997) 2045.
[3] T. Brousse, R. Retoux, U. Herterich, D.M. Schleich, J. Electrochem. Soc. 145 (1998) 1.
[4] Y. Idota, M. Mishima, Y. Miyiaki, T. Kubota, T. Miyasaka, Eur. Patent Appl. 651450 A1 94116643.1, 1994.
[5] Y. Idota, M. Mishima, Y. Miyiaki, T. Kubota, T. Miyasaka, US Patent 5,618,640 (1997).
[6] G.R. Goward, N.J. Taylor, D.C.S. Souza, L.F. Nazar, J. Alloys Compd. 329 (2001) 82.
[7] C.J. Wen, R.A. Huggins, J. Solid State Chem. 35 (1980) 376.
[8] A. Hightower, P. Delcroix, G. Le Caër, C.-K. Huang, B.V. Ratnakumar, C.C. Ahn, B. Fultz, J. Electrochem. Soc. 147 (2000) 1.
[9] I.A. Courtney, R.A. Dunlap, J.R. Dahn, Electrochim. Acta 45 (1999) 51.
[10] J. Chouvin, J. Olivier-Fourcade, J.C. Jumas, B. Simon, O. Godiveau, Chem. Phys. Lett. 308 (1999) 413.
[11] I. Sandu, T. Brousse, J. Santos-Peña, M. Danot, D.M. Schleich, Ionics 8 (2002) 27.
[12] D. Guyomard, J.-M. Tarascon, US Patent 5,192,629 (1993).
[13] M. Danot, A.M. Afanasov, I.S. Bezverkhyy, P.B. Fabritchnyi, J. Rouxel, Solid State Commun. 91 (1994) 675.
[14] N.N. Greenwood, T.C. Gibb, Mössbauer Spectroscopy, Chapman and Hall Ltd., London, 1971.
[15] M.S. Moreno, R.C. Mercader, Phys. Rev. B 50 (1994) 9875.
[16] R.A. Dunlap, D.A. Small, D.D. MacNeil, M.N. Obrovac, J.R. Dahn, J. Alloys Compd. 289 (1999) 135.
[17] G. Grube, E. Meyer, Z. Elektrochem. 40 (1934) 771;
D.M. Bailey, W.H. Skelton, J.F. Smith, J. Less-Common Met. 64 (1979) 233.
[18] M.V. Koudriachova, N.M. Harrison, S.W. de Leeuw, Solid State Ionics 157 (2003) 35.